

Single Polymer Photosensitizer for Tb^{3+} and Eu^{3+} Ions: An Approach for White Light Emission Based on Carboxylic-Functionalized Poly(*m*-phenylenevinylene)s

A. Balamurugan,[†] M. L. P. Reddy,^{*,†} and M. Jayakannan^{*,‡}

Chemical Sciences and Technology Division, National Institute for Interdisciplinary Science and Technology, Council of Scientific & Industrial Research (CSIR), Thiruvananthapuram-695019, Kerala, India, and Department of Chemistry, Indian Institute of Science Education and Research (IISER), NCL Innovation Park, Dr. Homi Bhabha Road, Pune 411008, India

Received: July 16, 2009; Revised Manuscript Received: August 21, 2009

Here, we have demonstrated a facile molecular approach to generate white light emission by combining carboxylic functionalized poly(*m*-phenylenevinylene)s polymeric architectures with lanthanide β -diketonate complexes. The new class of carboxylic functional conjugated polymeric materials was custom-designed from phenyl propanoic and acetic acids and structurally characterized by NMR, FT-IR, and MALDI-TOF spectroscopic techniques. The designed conjugated polymers were employed for the synthesis of lanthanide complexes in the presence of acetyl acetone (acac) as coligand and investigated their photophysical properties. For comparison, carboxylic-anchored oligo-phenylenevinylene (OPV) was also designed, characterized, and utilized for the synthesis of lanthanide complexes in the presence of acetyl acetone as coligand. Investigations revealed that carboxylic functionalized polymeric material with Eu^{3+} - β -diketonate complex exhibits unique magenta emission when excited at 310 nm. On the other hand, carboxylic functionalized polymeric material with Tb^{3+} - β -diketonate complex shows bright sky-blue emission. Interestingly, when Eu^{3+} and Tb^{3+} were incorporated into polymer backbone in equimolar ratio along with acetyl acetone as coligand, exhibited a white emission with CIE 1976 color coordinates $x = 0.28$, $y = 0.34$. The intrinsic quantum yield and lifetime of Ln^{3+} complexes have been evaluated. The singlet and triplet energy levels of the antenna chromophore ligands have been calculated and the probable energy transfer mechanisms in Ln^{3+} complexes have also been discussed. The effect of polymer structure and spacer effect on the photosensitizing of Tb^{3+} and Eu^{3+} ions was also investigated.

Introduction

Polymer light-emitting diodes (PLEDs) have been widely investigated since the first successful design of a functional diode using a conjugated polymer as the electroluminescent material in 1990.¹ Conjugated polymers exhibit several unique electrical and optical properties, easy fabrication as uniform films, and mechanical flexibility, as compared to inorganic electroluminescent materials.² Though the conjugated polymers have been successfully demonstrated for electroluminescent devices, many issues such as low luminescence intensity and lifetime, π -stack induced aggregated quenching, low quantum efficiency, and poor color purity are some of the unresolved problems.³ The use of polymers with lanthanide complexes that covalently bond in the main chain or as pendant groups will help to overcome the above drawbacks.⁴ The fascinating optical properties of lanthanide ions have promoted the use of such complexes in a wide variety of technological applications ranging from biomedical analysis to materials science.^{5,6} However, since f-f transitions are forbidden, free luminescent lanthanide cations have extremely low extinction coefficients and direct lanthanide excitation results only in modest luminescent intensities. To obviate this problem, organic ligands with large molar absorption coefficients can be coordinated to the lanthanide ion, resulting in sensitized emission by means of the so-called “antenna

effect”.⁷ The mechanism of antenna sensitization can be approximated by three differing steps, the initial excitation of the ligand, followed by intersystem crossing to give an excited triplet state, and then subsequent energy transfer to yield the metal centered excited state, which emits light. Among a host of organic ligands, the β -diketones⁸ and aromatic carboxylates⁹ are the most frequently used sensitizing ligands for enhancing lanthanide luminescence because they can chelate effectively to lanthanide cations. Interesting luminescent properties featuring either dual emission or binomial mode emission have been reported to result from the incorporation of two different lanthanides into a single molecular scaffold.¹⁰ However, many of the low-molecular-weight lanthanide complexes undergo decomposition to some extent during film formation by vacuum deposition. Decomposition of the lanthanide complexes can be avoided in spin-coated films containing the lanthanide complexes dispersed in polymer matrices.¹¹ A drawback of this technique is that nonuniform blending or dispersion of the dopants may result in phase separation and ionic aggregation.¹² The use of polymers with the lanthanide complexes covalently bonded in the main chain or as pendant groups will help to overcome the above-mentioned problems. Further, energy transfer in a covalently bound system will be effective due to the close proximity of the two components. Many studies have been focused on polymer systems doped or blended with lanthanide complexes.¹³ However, blending may not give rise to uniformly disperse and thermodynamically stable compositions. π -Conjugated polymers or poly(methylmethacrylate) bearing phenanthroline, bipyrlyridyl, binaphthyls, terpyridine,

* To whom correspondence should be addressed. E-mail: (M.J.) jayakannan@iiserpune.ac.in; (M.L.P.R.) mlreddy55@gmail.com.

[†] National Institute for Interdisciplinary Science and Technology.

[‡] Indian Institute of Science Education and Research (IISER).

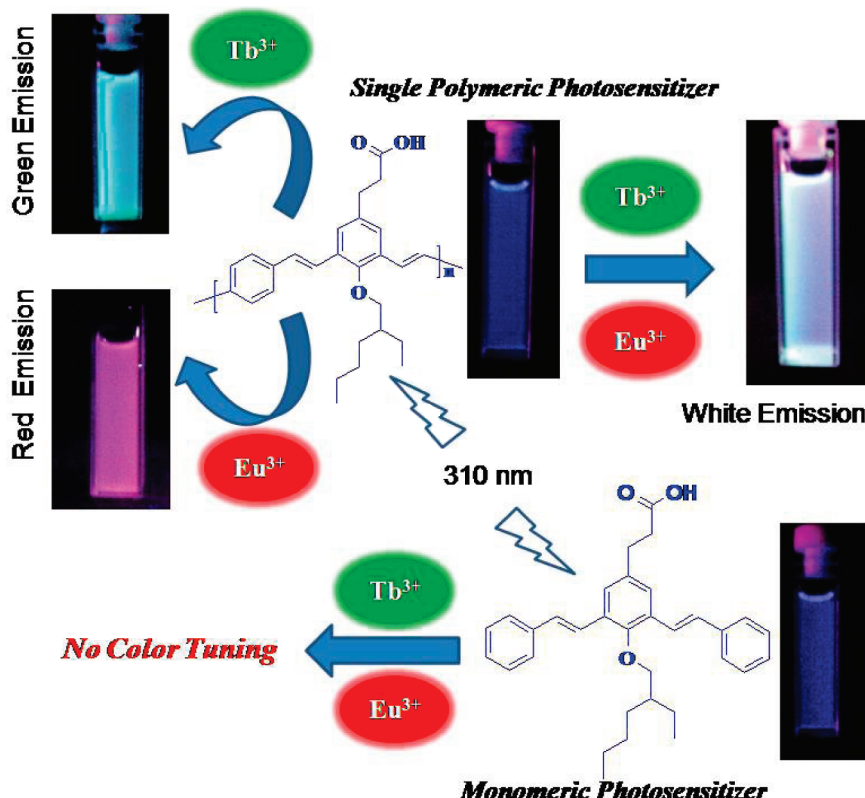


Figure 1. Single polymer based photosensitizer for tuning of emission colors in Ln^{3+} complexes.

*N,N'*diphenylenamine, polyvinylpyrrolidone, and polyvinylcarbazole were reported for lanthanide metal ions.^{4,14} Recently, a novel white-light emission has been proposed from a two-emitting system comprising a blue-emitting dysprosium-chelated terpyridine-based polymer and a red-emitting ruthenium complex.¹⁵ Design of single π -conjugated polymer based highly selective photosensitizer for one or two lanthanide metal ions (Eu^{3+} and Tb^{3+}) is a very attractive approach because (i) selective photosensitizing to either Tb^{3+} or Eu^{3+} can be utilized for sharp and bright green and red emission, (ii) partial self-emission of conjugated polymer may be used as a third primary color for the white emission, and (iii) fundamental understanding of color tuning and mechanistic aspects of energy transfer process in single polymeric systems-lanthanide complexes are not known. To the best of our knowledge, there is no report for single π -conjugated polymer based photosensitizer for white light emission from lanthanide ions.

These factors have prompted us to design a carboxylic functionalized poly(*m*-phenylenevinylene)s (m-PPV) for the selective color tuning of red, green, and white light emissions, which is a first of its kind based on a single polymeric photosensitizer for lanthanide complexes. Novel π -conjugated materials based on carboxylic functionalized poly(*m*-phenylenevinylene)s (m-PPV)s and oligo-phenylenevinylene (OPV) from phenyl propanoic or acetic acid and successfully employed as a suitable photosensitizer for Eu^{3+} and Tb^{3+} ions (see Figure 1). The newly designed conjugated polymer was found very superior in sensitizing Eu^{3+} or Tb^{3+} ions for sharp magenta and sky blue emissions, respectively, in the presence of acetylacetone as coligand. The partial self-emission from m-PPV conjugated backbone (blue) in combination with Eu^{3+} (magenta) and Tb^{3+} (sky blue) was cleverly utilized to obtain pure white light emitting materials. Further, the effect of spacer length between the metal centers to conjugated backbone and influence of copolymer on the photoexcitation process were also investigated.

Experimental Methods

Materials. 3-(4-Hydroxyphenyl)propanoic acid, 2-ethylhexylbromide, triethylphosphite, benzaldehyde, terephthaldehyde, isophthaldehyde, potassium-*tert*-butoxide, acetylacetone, $Gd(NO_3)_3 \cdot 6H_2O$, $Tb(NO_3)_3 \cdot 6H_2O$, and $Eu(NO_3)_3 \cdot 6H_2O$ were purchased from Aldrich chemicals. HBr in glacial acetic acid, paraformaldehyde, and all other reagents and solvents were purchased locally and purified following the standard procedure.

General Procedures. 1H NMR spectra of the compounds and the polymers were recorded using 300 and 500 MHz Bruker NMR spectrophotometer in $CDCl_3$ containing small amount of TMS as internal standard. Infrared spectra of the polymers and complexes were recorded using Perkin-Elmer Fourier transform infrared (FTIR) spectrophotometer. The purity of the monomers, intermediate compounds, and oligomer were determined by JEOL JSM600 fast atom bombardment (FAB) high-resolution spectrometry (HRMS) by dissolving the compound in THF and suspended in 3-nitrobenzyl alcohol as a matrix for FAB mass measurements. Elemental analysis was carried out using Elemental Vario EL-III CHN analyzer. The molecular weight of the polymer was determined by gel permeation chromatography (GPC) in tetrahydrofuran using polystyrene as standards. The flow rate of THF was maintained as 1 mL/min. The polymer solution was prepared by dissolving 3 mg of the sample in 1 mL of THF, filtered and injected for recording the GPC chromatograms. The chromatograms are recorded using waters 510 pump and detectors of waters 2487 UV-vis detector and waters 410 differential RI detector. Three mixed styra-gel columns in series HT 6E, HR 5E, and HR 4E are employed for separation. The thermal stability of the polymeric complexes was determined using TGA-50 Shimadzu thermogravimetric analyzer at a heating rate of 10 °C/min in nitrogen atmosphere. The absorption and emission studies were done by a Perkin-Elmer Lambda 35 UV-visible spectrophotometer and SPEX

Fluorolog DM-3000F spectrofluorimeter with a double-grating 0.22 m Spex 1680 monochromator and a 450 W Xe lamp as the excitation source using front face mode at room temperature. The solution spectra were recorded in THF and for solid state spectra polymers thin films were prepared by drop casting THF on quartz substrates. The concentrations of the polymer and standard solution were adjusted in such a way to obtain the absorbance equal to 0.1 at 310 nm. The excitation and emission spectra of the complexes were corrected at instrumental function.

Synthesis of Methyl 3-(4-hydroxyphenyl)propanoate (1). 3-(4-Hydroxyphenyl)propanoic acid (20 g, 120 mmol) was dissolved in dry methanol (100 mL). Concentrated H₂SO₄ (13 mL) was slowly added into the methanol solution with stirring and the content was refluxed for 24 h. The solvent was evaporated and the concentrated solution was poured into water. It was extracted with dichloromethane and the organic layer was washed with 5% NaHCO₃ solution and then with distilled water. After drying over Na₂SO₄, the solvent was evaporated to get colorless viscous liquid as the product. It was purified by silica gel column chromatography using 10% ethyl acetate and hexane. Yield = 19.6 g (91%). ¹H NMR (in CDCl₃) δ: 7.34 (s, 1H, Ar—OH), 6.99 (d, 2H, Ar—H), 6.76 (d, 2H, Ar—H), 3.64 (s, 3H, —CH₂—COOCH₃), 2.84 (t, 2H, Ar—CH₂CH₂), 2.58 (t, 2H, CH₂—CH₂COOCH₃). ¹³C NMR (in CDCl₃) δ: 174.56, 154.48, 131.97, 129.36 (2C), 115.49 (2C), 51.93, 36.12, and 30.08. FT-IR (cm⁻¹): 3393, 3022, 2953, 2863, 2699, 1885, 1738, 1713, 1614, 1597, 1516, 1440, 1363, 1297, 1220, 1211, 1173, 1103, 1028, 987, 952, 904, 830, 734, 551, 534, 497, and 459. HR-MS: MW = 180.21 and *m/z* = 180.06.

Synthesis of Methyl 3-(4-(2-ethylhexyloxy) phenyl)propanoate (2). Compound 1 (15 g, 83.3 mmol) and anhydrous K₂CO₃ (34.5 g, 2.5 mmol) were taken in flask containing dry DMF (60 mL) and stirred well at 75 °C under nitrogen atmosphere about 1 h. The catalytic amount of KI and 2-ethylhexyl bromide (17.7 g, 16.3 mL, 91.7 mmol) were added into the reaction mixture. The reaction was continued about 24 h at 80 °C under nitrogen atmosphere. The solvent was removed by vacuum distillation, and the residue was poured into the water and then extracted with dichloromethane. The organic layer was washed with 5% NaOH, brine solution, water, and then dried over Na₂SO₄. The solvent was evaporated to get yellow liquid as product. It was purified by passing through silica gel column using hexane +10% ethyl acetate. Yield = 16.9 g (70%). ¹H NMR (in CDCl₃) δ: 6.81 (d, 2H, Ar—H), 7.08 (d, 2H, Ar—H), 3.79 (d, 2H, Ar—OCH₂), 3.64 (s, 3H, —CH₂—COOCH₃), 2.87 (t, 2H, Ar—CH₂CH₂), 2.58 (t, 2H, CH₂—CH₂COOCH₃), 1.72–0.89 (m, 20H, aliphatic H). ¹³C NMR (in CDCl₃) δ: 173.44, 157.92, 132.26, 129.33, 129.14, 114.53, 114.32, 70.44, 51.54, 39.41, 36.04, 30.13, 29.10, 23.83, 23.08, 22.98, 14.1, and 11.11. FT-IR (cm⁻¹): 2961, 2927, 2874, 2859, 1739, 1613, 1582, 1513, 1463, 1436, 1364, 1296, 1245, 1174, 1107, 1034, 987, 825, and 770. HR-MS: MW = 292.24 and *m/z* = 292.24.

Synthesis of 3-(3,5-Bis(bromomethyl)-4-(2-ethylhexyloxy)phenyl)propanoic acid (3). Compound 2 (10 g, 34.2 mmol) and paraformaldehyde (3.1 g, 122.0 mmol) were taken in flask containing glacial acetic acid (40 mL). HBr in glacial acetic acid (8.5 mL, 30–33 wt %) was added dropwise to the above solution at room temperature and stirred for 0.5 h under N₂ atmosphere. It was gradually heated to 80 °C and stirred for 24 h. The reaction mixture was cooled to room temperature and second batch of paraformaldehyde (3.1 g, 122.0 mmol) and HBr in glacial acetic acid (8.5 mL, 30–33 wt %) were added. It was further carried out for 24 h by heating at 80 °C. The reaction mixture was cooled to room temperature and poured

into ice cold water. The precipitate was filtered and washed with water to completely remove acid impurities. The precipitate was dried in vacuum oven at 45 °C. Further the purification was done by recrystallization from hexane and dichloromethane mixture and the product was obtained as crystalline solid. Yield = 9.5 g (60%). ¹H NMR (in CDCl₃) δ: 7.21 (s, 2H, Ar—H), 4.50 (s, 4H, Ar—CH₂—Br), 3.96 (d, 2H, Ar—OCH₂), 2.90 (t, 2H, Ar—CH₂CH₂), 2.67 (t, 2H, —CH₂CH₂—COOH), 1.84–0.09 (m, 20H, Aliphatic H). ¹³C NMR (in CDCl₃) δ: 178.10, 154.12, 136.70, 132.07 (2C), 132.03 (2C), 77.51 (2C), 40.66, 35.22, 30.15, 29.70, 29.12, 27.64, 23.63, 23.11, 14.12, and 11.28. FT-IR (cm⁻¹): 2959, 2931, 2873, 2861, 1712, 1470, 1385, 1241, 1213, 1162, 1116, 1001, 916, 879, 585, and 515. HR-MS: MW = 464.24 and *m/z* = 464.20.

Synthesis of 3-(3,5-Bis(diethoxyphosphorylmethyl)-4-(2-ethylhexyloxy)phenyl)propanoic acid (4). Compound 3 (9 g, 19.4 mmol) and triethylphosphite (6.5 g, 38.8 mmol) (6.6 mL) were heated about 120–140 °C about 12 h under N₂ atmosphere. The excess triethylphosphite was removed by vacuum distillation to obtain the ylide as thick oil. It was purified by silica gel column chromatography using 20% ethyl acetate in hexane. Yield = 11.0 g (98%). ¹H NMR (in CDCl₃) δ: 7.22 (s, 2H, Ar—H), 4.02–4.13 (q, 8H, —PO(OCH₂CH₃)₂), 3.71 (d, 2H, Ar—OCH₂), 3.16–3.23 (d, 4H, Ar—CH₂PO—), 2.85–2.88 (t, 2H, Ar—CH₂CH₂), 2.59–2.61 (t, 2H, CH₂—CH₂COOH), 0.92–1.58 ppm (m, 32H, aliphatic H). ¹³C NMR (in CDCl₃) δ: 175.56, 153.98, 136.34, 130.09, 129.96, 124.87, 63.71, 62.51, 62.39, 62.34, 62.19, 61.60, 57.99, 53.43, 40.56, 35.76, 30.33, 30.12, 29.04, 27.16, 26.04, 23.48, 23.06, 20.87, 18.12, 16.29, and 14.16. FT-IR: 3148, 2964, 2928, 2871, 1728, 1618, 1474, 1396, 1247, 1163, 1022, 966, 880, 856, 781, 727, 622, 571, 534, 526, 500, 481, and 492. HR-MS: MW = 578.63 and *m/z* = 577.80.

Synthesis of 3-(4-(2-Ethylhexyloxy)-3,5-di(E)-styrylphenyl)propanoic acid (OPV) (5). Compound 4 (3 g, 5.2 mmol) and benzaldehyde (1.2 g, 11.3 mmol) were dissolved in dry THF (40 mL) and potassium tert-butoxide (15 mL, 1 M THF) was added and the contents were stirred under nitrogen atmosphere for 12 h at room temperature. It was poured into cold water (the residue was completely soluble in water) and neutralized with 10% HCl. The white precipitate was filtered and washed with water, dried in vacuum oven at 40 °C. The crude product was purified by passing through a silica gel column using 10% ethyl acetate and hexane (2:10 v/v) as eluent. Yield = 2.1 g (98%). ¹H NMR (in CDCl₃) δ: 7.55–7.06 (m, 16H, Ar—H and vinylic H), 3.71–3.70 (d, 2H Ar—O—CH₂), 2.98–2.96 (t, 2H, Ar—CH₂CH₂), 2.77–2.72 (t, 2H, CH₂—CH₂COOH), 1.80–0.85 (m, 32H, aliphatic H). ¹³C NMR (in CDCl₃) δ: 178, 153.66, 137.57, 135.91, 133.77, 131.34 (2C), 130.19, 129.66, 128.70, 128.49 (4C), 127.66 (2C), 126.55 (4C), 125.26 (2C), 123.16 (2C), 40.96, 35.75, 30.82, 30.45, 29.41, 23.83, 23.15, 14.08, 11.39. FT-IR (cm⁻¹): 3431, 3026, 2964, 2934, 2862, 1708, 1597, 1496, 1453, 1442, 1382, 1303, 1256, 1205, 1140, 1074, 968 (CH=CH, trans) 870, (CH=CH, cis) 848, 812, 743, 690, 532, 504. HR-MS MW = 482.67 and *m/z* = 482.71, 505.73 (M⁺ + Na⁺).

Synthesis of Poly[3-(4-(2-ethylhexyloxy)phenylenevinylene)-alt-(1,3-phenylenevinylene)propanoic acid] (m-PPV) (6). Compound 4 (1 g, 0.0017 mol) and isophthaldehyde (0.23 g, 1.73 mmol) were dissolved in dry THF (50 mL). The mixture was stirred well under nitrogen atmosphere about 15 min at room temperature. Potassium tert-butoxide (10.4 mL in 1 M THF) was added dropwise and stirred for further 12 h at room temperature under nitrogen atmosphere. It was poured into water

and neutralized with 10% HCl, the product was washed with excess of water. The sticky product was purified by washing with water and methanol. It was dried in a vacuum oven at 40 °C for 5 h prior to further analysis. Yield = 0.36 g (51%). ¹H NMR (in CDCl₃) δ: 7.52–7.04 (m, 10H, Ar–H and vinylic H), 3.69–3.68 (d, 2H –O–CH₂), 2.97–2.95 (t, 2H, Ar–CH₂CH₂), 2.75–2.72 (t, 2H, CH₂–CH₂COOH), 1.90–0.82 (m, 32H, aliphatic H). ¹³C NMR (in CDCl₃) δ: 173.20, 153.65, 133.73, 130.15, 129.09, 128.76, 127.75, 125.36, 124.25, 123.92, 40.01, 29.84, 29.58, 29.31, 28.65, 28.15, 27.83, 26.51, 26.19, 25.93, 25.07, 22.75, 20.89, 15.27, 14.17, 13.05, 10.20, and 9.30. FT-IR (cm⁻¹): 3450, 2959, 2933, 2866, 1721, 1600, 1597, 1463, 1347, 1250, 1216, 1156, 1046, 971 (CH=CH, trans), 856 (CH=CH, cis) 795 and 498. Molecular weight (GPC, in THF): M_n = 2700 and M_w = 3300.

Synthesis of Ln(acac)₃(OPV) (Ln = Eu³⁺ or Tb³⁺). To an ethanolic solution of OPV (0.15 g, 0.31 mmol), NaOH (0.014 g, 0.342 mmol) solution was added, the mixture was stirred for 5 min. To this a saturated ethanolic solution, in situ prepared Ln(acac)₃ is added dropwise and the stirred for 10 h. Water is then added into this mixture and precipitate thus formed is filtered, washed with water, and dried. It was further purified by recrystallization from dichloromethane–ethanol mixture.

Synthesis of Ln(acac)₃(H₂O) (Ln = Eu³⁺ or Tb³⁺). Acetyl acetone (0.099 g, 0.99 mmol) was dissolved in dry ethanol (5 mL) and NaOH (0.052 g, 1.30 mmol) in water (2 mL) was added into the mixture. The whole mixture was stirred well about 1/2 h to become a clear solution at room temperature and then Ln(NO₃)₃·6H₂O (0.15 g, 0.341 mmol) in dry ethanol (3 mL) was added into the reaction mixture.

Eu(acac)₃(H₂O)(OPV). FT-IR (cm⁻¹): 3460, 2924, 1521, 1498, 1405, 1390, 1254, 1218, 1151, 1079, 1014, 975, 946, 920, 846, 731, 694, 660, 643, and 512. Anal. Calcd. for C₄₈H₆₄O₁₀Eu: C, 60.50; H, 6.77. Found: C, 60.71; H, 7.26. *m/z* = 950.60.

Tb(acac)₃(H₂O)(OPV). FT-IR (cm⁻¹): 3438, 2964, 2935, 2869, 1605, 1517, 1450, 1318, 1274, 1208, 1172, 1080, 1033, 985, 802, 754, 728, 593, 571, and 543. Anal. Calcd. for C₄₈H₆₄O₁₀Tb: C, 60.06; H, 6.72. Found: C, 59.65; H, 6.47. *m/z* = 956.64.

Synthesis of Gd(OPV)₃2(H₂O). An aqueous solution of Gd(NO₃)₃·6H₂O (0.03 g, 0.067 mmol) was added to a solution of OPV (0.1 g, 0.21 mmol) in ethanol in the presence of NaOH (0.02 g, 0.64 mmol). Precipitation took place immediately, and the reaction mixture was stirred for 10 h at room temperature. The product was filtered, washed with ethanol, water, and ethanol, and then dried. The complex was then purified by recrystallization from dichloromethane–ethanol mixture. FT-IR (cm⁻¹): 3436, 2970, 2928, 2872, 1596, 1537, 1498, 1454, 1315, 1258, 1208, 1136, 1000, 963, 873, 847, 737, 688, and 529. Anal. Calcd. for C₉₉H₈₅O₁₁Gd: C, 72.45; H, 7.25. Found: C, 72.05; H, 7.48. *m/z* = 1638.33.

Synthesis of Eu(acac)₃(m-PPV) and Tb(acac)₃(m-PPV) Complexes. To the THF solution of m-PPV (0.05 g, 0.123 mmol), NaOH (0.005 g, 0.123 mmol) solution was added, the mixture was stirred for 5 min. To this a saturated THF solution in situ prepared Ln(acac)₃ is added dropwise and the stirred for 12 h. Water is then added into this mixture and precipitate thus formed is filtered, washed with water, and dried under vacuum at 50 °C.

Eu(acac)₃(m-PPV). FT-IR (cm⁻¹): 3421, 2967, 2917, 1597, 1519, 1466, 1412, 1259, 1194, 1016, 918, 782, 760, 657, 627, 573, 525, and 483.

Tb(acac)₃(m-PPV). FT-IR (cm⁻¹): 3420, 2964, 2923, 2859, 1560, 1522, 1446, 1413, 1300, 1254, 1202, 1880, 1166, 1045,

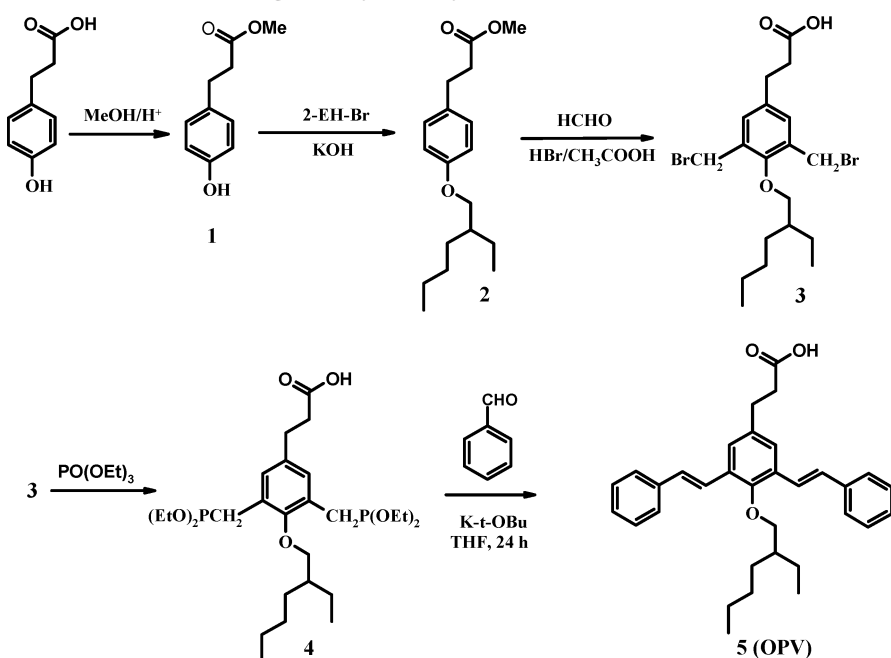
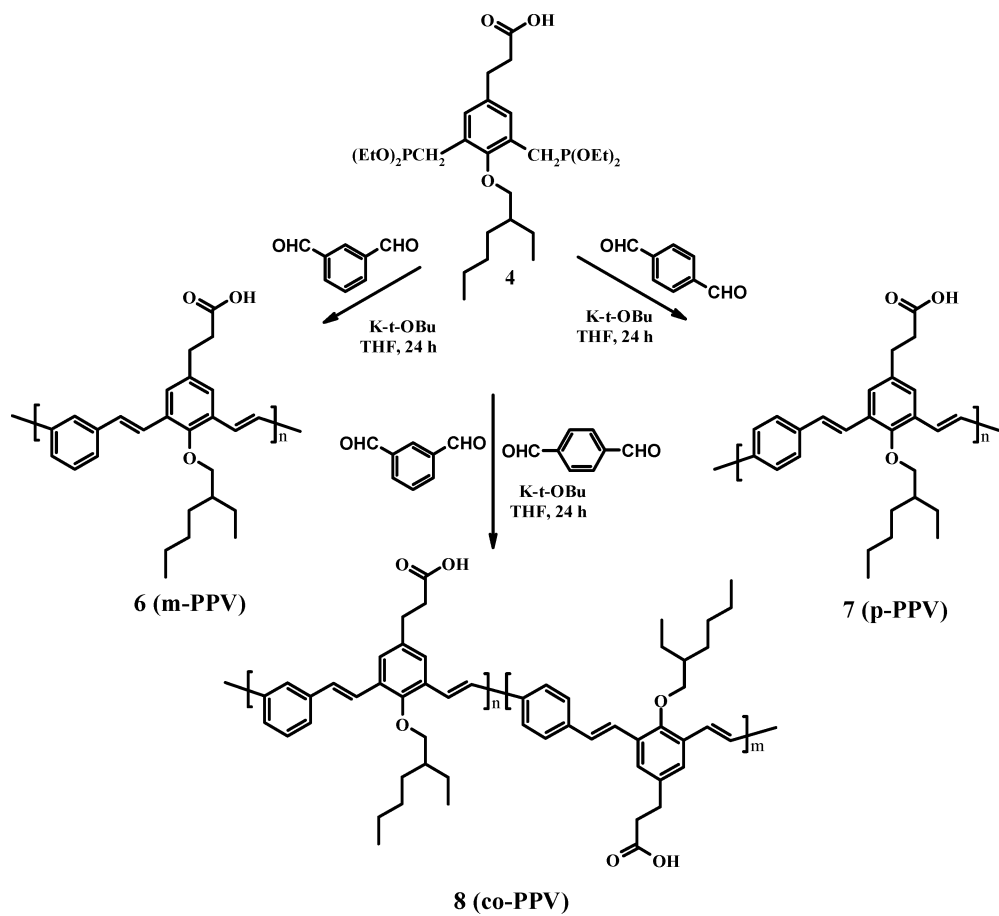
968, 916, 847, 981, 688, and 532. Similar procedure was adopted for the synthesis of other co-PPV, p-PPV complexes.

Gd(m-PPV)(NO₃)₂. FT-IR (cm⁻¹): 3392, 2928, 1559, 1451, 1416, 1311, 1256, 1201, 1188, 1049, 1075, 1046, 960, 847, 772, 788, 694, 617, 569, 526, 504, and 486.

Synthesis of Eu_{0.5}Tb_{0.5}(acac)₃(m-PPV). To the THF solution of m-PPV (0.05 g, 0.123 mmol), NaOH (0.005 g, 0.123 mmol) solution was added, the mixture was stirred for 5 min. To this a saturated THF solution, in situ prepared Eu_{0.5}Tb_{0.5}(acac)₃ is added dropwise and the stirred for 12 h. Water is then added into this mixture and the precipitate thus formed is filtered, washed with water, and dried under vacuum at 50 °C. Eu_{0.5}Tb_{0.5}(acac)₃(m-PPV): FT-IR (cm⁻¹): 3426, 2956, 2927, 2857, 1599, 1519, 1404, 1260, 1277, 1157, 1022, 963, 916, 847, 763, 655, 529, and 488. The 1:1 molar ratios of Eu³⁺/Tb³⁺ in Eu_{0.5}Tb_{0.5}(acac)₃(m-PPV) and Eu_{0.5}Tb_{0.5}(acac)₃(m-PPV-A) were confirmed by EDS analyses (Figure S12–S13 and Table S1, Supporting Information).

Results and Discussions

Synthesis of Polymers and Ln³⁺ Complexes. The carboxylic functionalized monomer was designed from commercially available 3-(4-hydroxyphenyl)propanoic acid and was converted into required bis-ylide monomer and oligo(phenylenevinylene) (OPV) model compound as shown in Scheme 1. Methyl-3-(4-hydroxyphenyl)propanoate (**1**) was prepared by refluxing 3-(4-hydroxyphenyl)propanoic acid with methanol and concentrated H₂SO₄. 2-Ethylhexyl bromide was reacted with **1** in K₂CO₃/DMF under nitrogen atmosphere to get methyl-3-(4-(2-ethylhexyloxy)phenyl)propanoate (**2**). **2** was bis-bromomethylated with *p*-formaldehyde in the presence of HBr/acetic acid to yield 3-(3,5-bis(bromomethyl)-4-(2-ethylhexyloxy)phenyl)propanoic acid (**3**). **3** was converted into bis-ylide 3-(3,5-bis((diethoxyphosphoryl)methyl)-4-(2-ethylhexyloxy)phenyl)propanoic acid (**4**). The bis-ylide monomer (**3**) was polymerized with isophthaldehyde and terephthaldehyde under Wittig–Horner reaction conditions in the presence of potassium *tert*-butoxide as the base to yield poly[3-(4-(2-ethylhexyloxy)phenylenevinylene)-alt-(1,3-phenylenevinylene)] (**m-PPV**) and its para counterpart poly[3-(4-(2-ethylhexyloxy) phenylenevinylene)-alt-(1,4-phenylenevinylene)] (**p-PPV**), respectively (see Scheme 2). A copolymer (**co-PPV**) bearing 50:50% of *p*- and *m*-content was prepared by polymerizing **3** with equal mole ratio of terephthaldehyde and isophthaldehyde under the same conditions. A structurally identical model compound 3-(4-(2-ethylhexyloxy)-3,5-di(E)-styrylphenyl)propanoic acid (**OPV**) was prepared by reacting **3** with two moles of benzaldehyde (see Scheme 1). The structures of the monomers, OPV, and polymer were characterized by ¹H, ¹³C NMR, FT-IR and FAB-HRMS (Figures S1–S10, Supporting Information). The ¹H NMR spectra of the **m-PPV** polymer and **OPV** were shown in Figure 2 and different types of protons in the structure were assigned by alphabets. In Figure 2a, the OPV has three peaks at 3.70, 3.00, 2.75 ppm corresponding to Ar–OCH₂–, Ar–CH₂CH₂, and CH₂–CH₂COOH, respectively. The multiple of peaks above 7.00 ppm were assigned to aromatic and vinylene protons that were matching with that of expected structure as reported earlier. In Figure 2b, the m-PPV polymer has also almost identical pattern of peaks except peaks for proton-b at 7.45 ppm with respect to its structure. The FT-IR spectra of the polymers and OPV (Figure S11, Supporting Information) showed characteristic peaks at 3450 and 3447 cm⁻¹ for O–H stretching of –COOH group, respectively. The peaks at 1721 and 1708 cm⁻¹ were assigned to C=O stretching of carboxylic acid groups in m-PPV and OPV, respectively. All other peaks at 2930, 1250, 1255 cm⁻¹ (C–O ether linkage),

SCHEME 1: Synthesis of Monomer and Oligo-Phenylenevinylene**SCHEME 2: Synthesis of Carboxylic Functionalized Poly(*m*-phenylenevinylene)s**

972, 970 cm^{-1} (trans, $\text{HC}=\text{CH}$), and 856, 870 cm^{-1} (cis $\text{HC}=\text{CH}$) vinylene C–H out-of-plane bending and the values are matching with that of the expected structure. The molecular weights were obtained $M_n = 2300\text{--}5300$ and $M_w = 3300\text{--}6900$ indicating the formation of moderate molecular weight polymers with an average of 9–10 repeating units in the polymer chain. In general, poly(*m*-phenylenevinylene)s were produced lower

molecular weights due to formation macrocyclic rings and also low degree of conversion in the bis-ylide Wittig polycondensation reactions.^{3f-j} Therefore, the molecular weights of the polymers reported here were typically accepted for bis-ylide condensation route. It is well-known that the photophysical properties of the conjugated polymers were almost invariant for 6–8 repeating units in the polymer chain. The synthesized

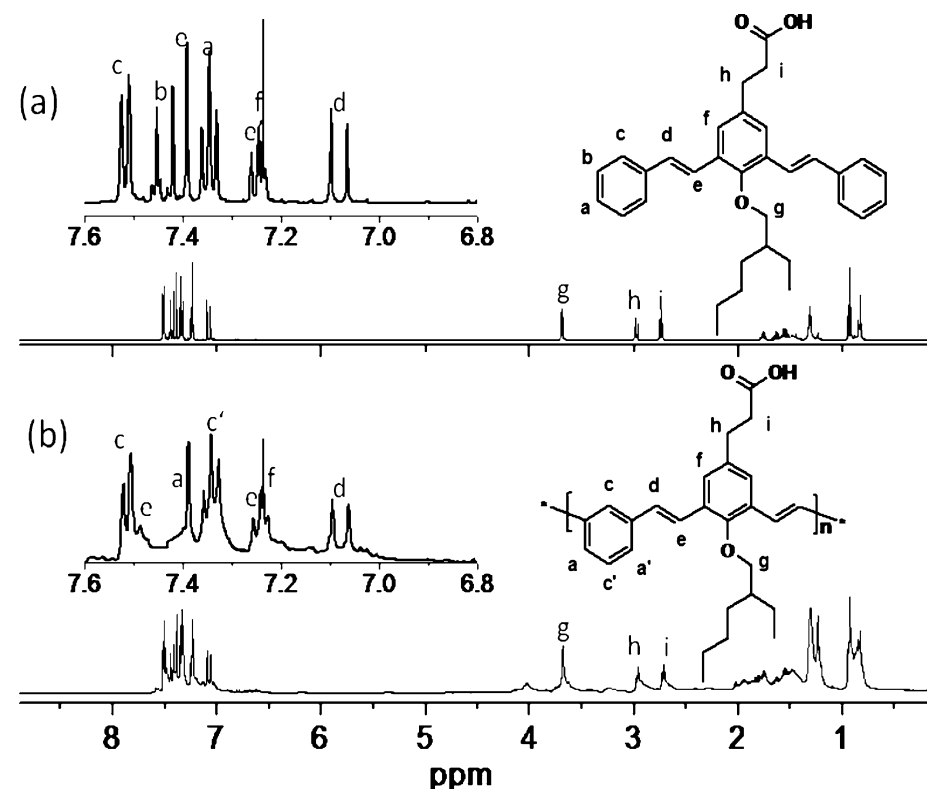


Figure 2. ^1H NMR Spectra of OPV and m-PPV in CDCl_3 .

polymers have an average of 16–20 aromatic rings in the backbone, and therefore the carboxylic functionalized polymers were sufficient enough for studying lanthanide metal ions complexation.

Newly designed carboxylic functionalized polymers (PPVs) and OPV were utilized as multidentate polymeric or small molecular ligands for the syntheses of Ln^{3+} complexes. Acetylacetone was used as coligand and the complexation was carried out in presence of ethanol using NaOH as base. One mole equivalence of $\text{Ln}(\text{NO}_3)_3 \cdot 6\text{H}_2\text{O}$ ($\text{Ln} = \text{Eu}^{3+}$ or Tb^{3+}) was reacted with three mole equivalents of acac in ethanol to form $\text{Ln}(\text{acac})_3$ (in situ preparation). The PPVs and OPV were converted into its sodium salts by reacting with NaOH in water. The sodium salt was added to the in situ prepared $\text{Ln}(\text{acac})_3$ solution. The complex $[\text{Ln}(\text{acac})_3(\text{OPV})$ or $\text{Ln}(\text{acac})_3(\text{PPV})]$ was precipitated from the reaction solution and it was filtered then washed with hot water/ethanol to get pure complexes. In the case of the OPV complexes, the precipitate was further purified by recrystallization from dichloromethane/ethanol mixture. The formations of the complexes were confirmed by FT-IR spectroscopic techniques (Figure S11, Supporting Information). The carbonyl stretching frequency at 1723 cm^{-1} (C=O stretching) in m-PPV vanished and new peaks appeared at 1601 and 1420 cm^{-1} corresponding to the antisymmetric and symmetric vibration of the M-C=O carboxylate group. The broad peak around 3400 – 3550 cm^{-1} shows that water molecules are also coordinated to the polymer complexes. Similarly formation OPV complexes were confirmed by the absence of carbonyl stretching frequency of the OPV at 1702 cm^{-1} and new peaks at 1603 and 1450 cm^{-1} are corresponding to the antisymmetric and symmetric vibration were observed. The molecular weights and structures of the OPV complexes were confirmed by MALDI-TOF analysis. In Figure 3a,b, the molecular ion peaks at 956.64 and 950.60 were matching with expected molecular weights of $\text{Tb}(\text{acac})_3(\text{OPV}) \cdot \text{H}_2\text{O}$ and $\text{Eu}(\text{acac})_3(\text{OPV}) \cdot \text{H}_2\text{O}$, respectively.

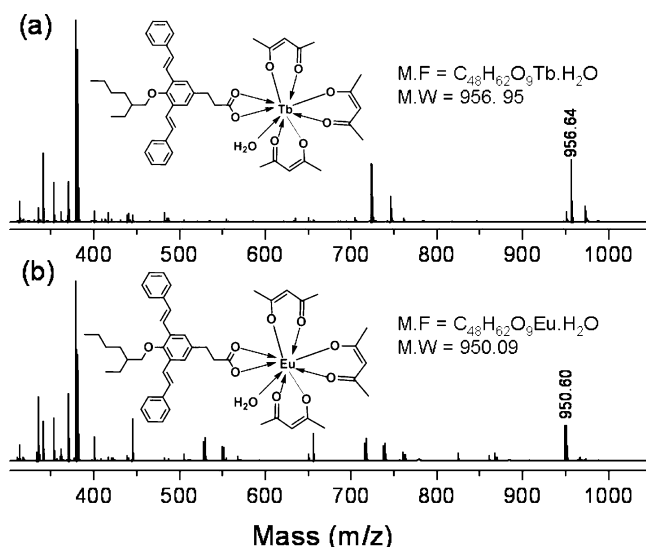


Figure 3. MALDI-TOF Spectra of $\text{Eu}(\text{acac})_3\text{OPV} \cdot \text{H}_2\text{O}$ and $\text{Tb}(\text{acac})_3\text{OPV} \cdot \text{H}_2\text{O}$ complexes.

It is clearly evident that the OPV molecule involved in the complex formation with $\text{Tb}(\text{acac})_3$ or $\text{Eu}(\text{acac})_3$. The 1:1 molar ratios of $\text{Eu}^{3+}/\text{Tb}^{3+}$ in $\text{Eu}_{0.5}\text{Tb}_{0.5}(\text{acac})_3(\text{m-PPV})$ ($\text{Eu}/\text{Tb} = 0.98$) and $\text{Eu}_{0.5}\text{Tb}_{0.5}(\text{acac})_3(\text{m-PPV-A})$ ($\text{Eu}/\text{Tb} = 1.17$) were confirmed by EDS analyses (Figure S12-S13 and Table S1, Supporting Information). From the thermogravimetric analysis data, it is clear that complexes $\text{Eu}(\text{acac})_3(\text{m-PPV})$, $\text{Tb}(\text{acac})_3(\text{m-PPV})$, and $\text{Eu}_{0.5}\text{Tb}_{0.5}(\text{acac})_3(\text{m-PPV})$ undergo weight loss of 5% up to 250°C , which corresponds to the elimination of coordinated water molecules. Further decomposition takes place in two steps and leaves the final residue of approximately 43%, which corresponds to the lanthanide oxides (Figure S14, Supporting Information).

Photophysical Properties. The absorption and emission spectra of OPV and m-PPV were recorded at 298 K for drop

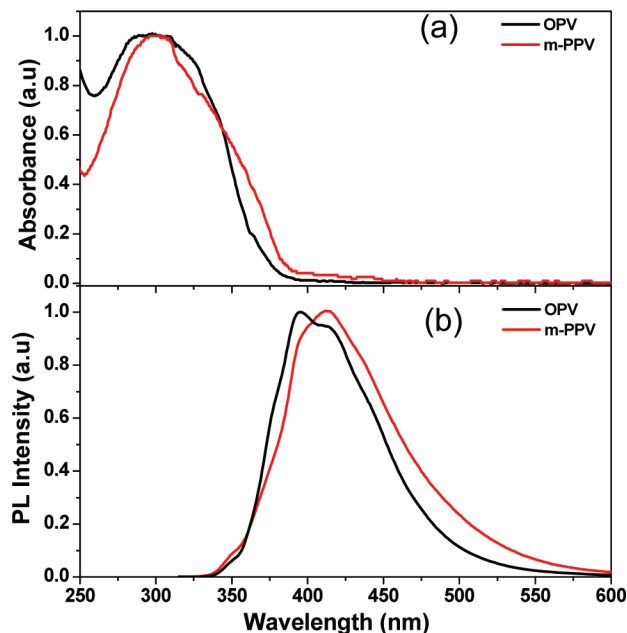


Figure 4. Absorption (a) and emission (b) spectra of OPV and m-PPV.

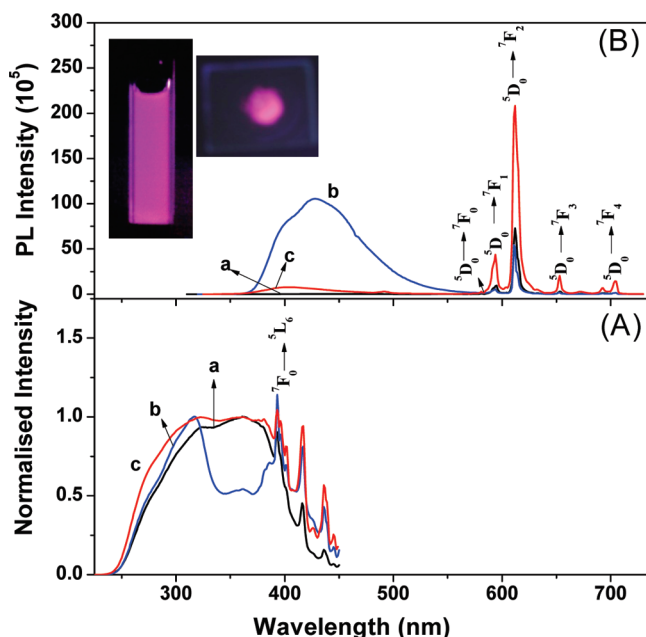


Figure 5. Excitation (A) and emission (B) spectra of Eu³⁺ complexes. Eu(acac)₃ (a); Eu(acac)₃(OPV) (b); Eu(acac)₃(m-PPV) (c).

casted films (on quartz plate) and are given in Figure 4. The absorption maximum of the m-PPV noted at 305 nm is attributed to the $\pi-\pi^*$ absorption of aromatic phenylene rings. The emission maximum of m-PPV was obtained as 412 nm. The absorption and emission peak maxima of OPV is same as that of m-PPV which provides an opportunity to investigate the effect of long chain and short oligomeric ligand in Ln³⁺ complexes without altering their band gaps. The normalized excitation spectra of the Eu³⁺ complexes, which was recorded at 298 K and monitored around the intense $^5D_0 \rightarrow ^7F_2$ transition of the Eu³⁺ cation, is shown in Figure 5A. The excitation spectra recorded for the metal-centered emission of the Eu³⁺ complex overlaps with the absorption spectra of ligands (OPV and m-PPV) in the region 250–400 nm. A series of sharp lines, which are assigned to transitions between the $^7F_{0,1}$ and $^5L_6, ^5D_{3-1}$

levels, are also evident in the excitation spectra of these complexes.¹⁶ However, these transitions are weaker than the absorptions due to the organic ligands and are overlapped by a broad excitation band, thus proving that luminescence sensitization that arises from excitation of the ligand is considerably more efficient than the direct excitation of the Eu³⁺ absorption level. The emission spectra of Eu³⁺ complexes (Figure 5B) excited at 310 nm exhibited the characteristic narrow bands arising from the intraconfigurational $^5D_0 \rightarrow ^7F_J$ ($J = 0-4$) transitions of the Eu³⁺ ion.¹⁶ The PL spectrum of the complexes dispersed in DMSO has also showed the emission from the metal center; however, its intensity is relatively less compared to that of the solid state. It is interesting to note that only a weak residual emission due to m-PPV is observed in Eu(acac)₃(m-PPV), indicating an efficient ligand-to-metal energy transfer process. On the other hand, in the case of Eu(acac)₃(OPV), the self-emission of OPV was also present indicating that OPV is a poor-sensitizer for Eu³⁺. In the case of Eu(acac)₃, only weak intraconfigurational $^5D_0 \rightarrow ^7F_J$ transitions of the Eu³⁺ ion is observed. The five narrow emission peaks centered at 579, 590, 612, 649, and 699 nm, assigned to $^5D_0 \rightarrow ^7F_0$, $^5D_0 \rightarrow ^7F_1$, $^5D_0 \rightarrow ^7F_2$, $^5D_0 \rightarrow ^7F_3$, and $^5D_0 \rightarrow ^7F_4$ transitions, respectively.^{8a,b,9a,16} Among the peaks, the emission at 612 nm from the $^5D_0 \rightarrow ^7F_2$ induced electronic dipole transition is the strongest, suggesting the chemical environment around Eu³⁺ ions does not have an inversion center.¹⁷ The relative energy-transfer efficiency in the OPV or m-PPV containing the Eu(acac)₃ complex is determined from the ratio of the maximum emission intensity of two chromophores ($I_{612}/I_{350-560}$, where I_{612} is the maximum intensity of main emission peak of Eu³⁺ complex at around 612 nm and $I_{350-560}$ is the maximum intensity of main emission peak of OPV or m-PPV in the range of 350–560 nm) (Table 1). As can be seen from Table 1 and Figure 5B, m-PPV has the highest energy-transfer efficiency in solid state compared to that of OPV. Thus the combination of strong red emissions from Eu³⁺ center at 612 nm and weak blue emissions in the region 375 to 450 nm due to the residual emission from m-PPV results in an interesting magenta-colored emission with CIE coordinates 0.33 and 0.17, when Eu(acac)₃(m-PPV) is excited at 310 nm.

To understand the energy transfer processes in the synthesized Eu³⁺ complexes, it was necessary to determine the singlet and triplet energy levels of the m-PPV and OPV. The singlet ($^1\pi \pi^*$) energy levels of these ligands were estimated by reference to the wavelengths of the UV-vis absorption edges of ligands. The relevant values were 395 nm (25 300 cm⁻¹), and 370 nm (27 000 cm⁻¹) for m-PPV and OPV, respectively (see Figure 4). The triplet energy levels ($^3\pi\pi^*$) of the ligands were calculated by reference to the lower wavelength emission edges (480 nm, 20800 cm⁻¹ and 448 nm, 22300 cm⁻¹ for m-PPV and OPV, respectively) from the low-temperature phosphorescence spectra of the Gd³⁺ complexes of the pertinent ligands (Figure S16, Supporting Information). Because there is a large energy gap (ca. 32 000 cm⁻¹) between the $^8S_{1/2}$ ground state and the first $^6P_{7/2}$ excited state of the Gd³⁺ ion, it cannot accept any energy from the first excited triplet state of the ligand via intramolecular ligand-to-metal energy transfer.¹⁸ Thus the phosphorescence spectra of Gd³⁺ complexes actually reveal the triplet energy levels ($^3\pi\pi^*$) of m-PPV and OPV in the Ln³⁺ complexes. It is well recognized that the energy-level match between the triplet state ($^3\pi\pi^*$) of the ligand to the 5D_0 state of the Eu³⁺ cation is one of the key factors that governs the luminescence efficiency of Eu³⁺ complexes.^{8a,c,g} Latva's empirical rule states that an optimal ligand-to-metal energy transfer process for Eu³⁺ requires ΔE ($^3\pi\pi^* - ^5D_0$) = 2500–4000 cm⁻¹

TABLE 1: Luminescence Intensity Ratio of the Complexes

| complexes | $I_{Tb}/I_{350-480}$ | $I_{Eu}/I_{350-560}$ | $A_{Tb}/A_{350-480}^a$ | $A_{Eu}/A_{350-560}^b$ |
|-------------------------------|----------------------|----------------------|------------------------|------------------------|
| $Eu(acac)_3$ (H_2O) (OPV) | | 0.52 | | 0.03 |
| $Eu(acac)_3$ (m-PPV) | | 22.13 | | 1.99 |
| $Tb(acac)_3(H_2O)$ (OPV) | 1.49 | | 0.23 | |
| $Tb(acac)_3$ (m-PPV) | 0.52 | | 0.11 | |

^a Area of emission peak at 547 nm (corresponding to Tb)/area of the sensitizer from 350–480 nm. ^b Area of emission peak at 612 nm (corresponding to Eu)/area of the sensitizer from 350–560 nm.

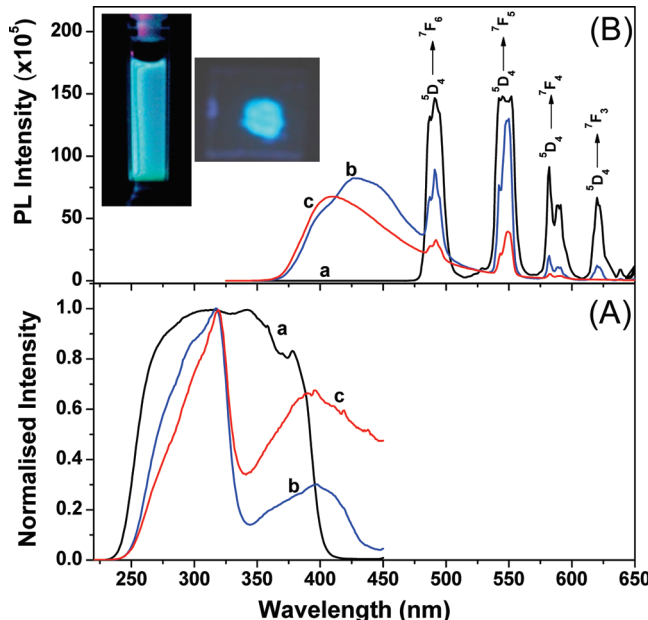


Figure 6. Excitation (A) and emission (B) spectra of Tb^{3+} complexes. $Tb(acac)_3$ (a); $Tb(acac)_3$ (OPV)(b); $Tb(acac)_3$ (m-PPV)(c).

for Eu^{3+} .¹⁹ On this basis, it can be concluded that the energy transfer to the Eu^{3+} cation will be more effective in the case of m-PPV than that of OPV, since ΔE ($^3\pi\pi^* - ^5D_0$) for $Eu(acac)_3$ (m-PPV) and $Eu(acac)_3$ (OPV) are 3300 and 4800 cm^{-1} , respectively. According to Reinhoudt's empirical rule, the intersystem crossing process becomes effective when ΔE ($^1\pi\pi^* - ^3\pi\pi^*$) is at least 5000 cm^{-1} .²⁰ The energy gaps ΔE ($^1\pi\pi^* - ^3\pi\pi^*$) for ligands m-PPV and OPV are 4500 and 4700 cm^{-1} , respectively. As a consequence, the intersystem crossing processes are effective for both of these chromophores.

The steady-state excitation and emission spectra of Tb^{3+} complexes at room temperature are shown in Figure 6. The excitation spectrum of the Tb^{3+} complexes monitored around the peak of the intense $^5D_4 \rightarrow ^7F_5$ transition of the Tb^{3+} ion exhibits a broadband between 250 and 450 nm with a maximum at approximately 310 nm and a shoulder at 370 nm (Figure 6A). The peak at 310 nm can be assigned to the $^1\pi - \pi^*$ transition of the aromatic ring and the shoulder at 370 nm is attributable to $^1\pi - \pi^*$ transition of the carbonyl group of the ligand. The room-temperature emission spectra of the Tb^{3+} complexes excited at their maximum excitation wavelengths (λ_{ex}) 310 nm exhibit the characteristic emission bands for Tb^{3+} -centered emission at 490 , 547 , 585 , and 620 nm , which result from deactivation of the 5D_4 excited state to the corresponding ground state 7F_J ($J = 6$, 5 , 4 , 3) of the Tb^{3+} ion.^{8b,d,9} The most intense emission is centered at 547 nm and corresponds to the $^5D_4 \rightarrow ^7F_5$ transition. The spectra of both $Tb(acac)_3(H_2O)$ (OPV) and $Tb(acac)_3$ (m-PPV) complexes showed a broad emission peak between 360 – 475 nm with respect to self-emission of the ligand chromophores. No emission bands from the acac ligand is observed in $Tb(acac)_3$ complex, thus implying efficient energy

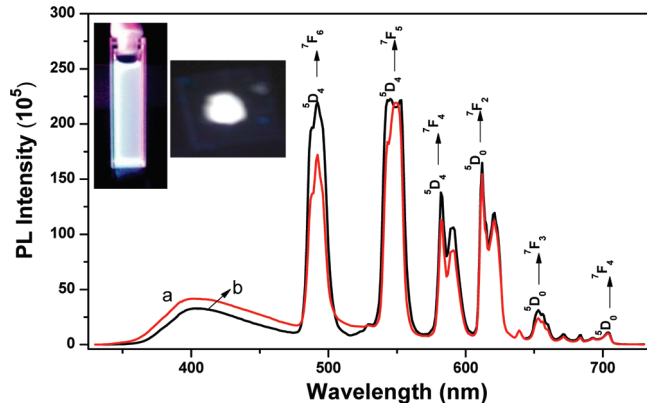
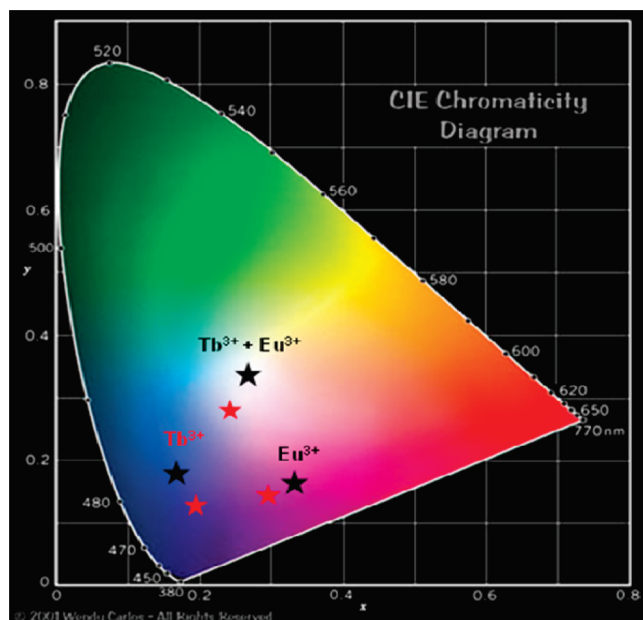


Figure 7. Emission spectra of (a) $Eu_{0.5}Tb_{0.5}(acac)_3$ (m-PPV) and (b) $Eu_{0.5}Tb_{0.5}(acac)_3$ (m-PPV-A) in solid state.

transfer from acac ligand to the central Tb^{3+} ion. Because of the superior match of the triplet energy level of acac ($23\ 800\text{ cm}^{-1}$)²¹ with that of the 5D_4 emitting level of Tb^{3+} ion efficient energy transfer takes place in $Tb(acac)_3$ complex ($\Delta E = ^3\pi\pi^* - ^5D_4 = 3400\text{ cm}^{-1}$). Because of the emission peaks in blue (375 to 475 nm of m-PPV polymer) and green (547 nm in view of $^5D_4 \rightarrow ^7F_5$ transitions of Tb^{3+}) regions, $Tb(acac)_3$ (m-PPV) exhibits interesting sky blue emission (Figure 6B) with CIE 1976 color coordinates 0.18 and 0.15 (Figure 6) when excited at 310 nm . On the other hand, $Tb(acac)_3$ (OPV) complex shows blue color when excited at 310 nm essentially due to the strong blue emission of the OPV in the region 360 – 475 nm . The energy transfer efficiency of various ligands in the case of Tb^{3+} follows the order acac ($\Delta E = 3400\text{ cm}^{-1}$) > OPV ($\Delta E = 1900\text{ cm}^{-1}$) > m-PPV ($\Delta E = 400\text{ cm}^{-1}$), which is also in the order of ratio ($I_{547}/I_{360-475}$, where I_{547} is the maximum intensity of main emission peak of Tb^{3+} complex at around 547 nm and $I_{360-475}$ is the maximum intensity of main emission peak of OPV or m-PPV in the range of 360 – 475 nm) of the maximum emission intensity peaks.

White Light Emission. Interestingly, when Eu^{3+} and Tb^{3+} were incorporated into m-PPV and m-PPV-A polymer backbone in equimolar ratio along with acetyl acetone as coligand, excitation of the resulting $Eu_{0.5}Tb_{0.5}(acac)_3$ (m-PPV) and $Eu_{0.5}Tb_{0.5}(acac)_3$ (m-PPV-A) compounds at 310 nm exhibited a novel white emission color (see Figure 7) with CIE 1976 color coordinates $x = 0.28$, $y = 0.34$ (Figure 8) and m-PPV-A ($x = 0.36$, $y = 0.38$) (Figure S17 in Supporting Information). The room-temperature emission spectra displays sharp emissions in the region at 490 , 547 , 585 , and 620 nm corresponding to $^5D_4 \rightarrow ^7F_J$ ($J = 6$, 5 , 4 , 3) transitions of Tb^{3+} ion and the peaks at 581 , 594 , 612 , 653 , 705 corresponding to transition of $^5D_0 \rightarrow ^7F_{J=0,1,2,3,4}$ of Eu^{3+} ion. In addition to the above sharp emissions, there also exists a broadband in the blue region (350 to 425 nm) due to the residual emission from the m-PPV polymer. The photograph of the $Eu_{0.5}Tb_{0.5}(acac)_3$ (m-PPV) was showed in Figure 7 which directly evident for the white emission in both powder and solution (dispersed in DMSO) states.



| Complexes | In solid | | In solution | |
|--|-------------|-------------|-------------|-------------|
| | X | Y | X | Y |
| Eu(acac)₃-m-PPV | 0.33 | 0.17 | 0.32 | 0.14 |
| Tb(acac)₃-m-PPV | 0.18 | 0.15 | 0.18 | 0.12 |
| Eu(acac)₃-m-PPV Tb(acac)₃ | 0.27 | 0.34 | 0.22 | 0.29 |

Figure 8. CIE color coordinates diagram of Ln^{3+} -m-PPV complexes in both solution and solid states.

Lifetime and Intrinsic Quantum Yield of Ln^{3+} Complexes. In addition to the steady-state emission spectra of Ln^{3+} complexes, the luminescent lifetimes of these complexes were measured at room temperature (298 K) from the respective luminescent decay profiles by fitting with monoexponential decay curves (Figure 9 and Figure S18 in Supporting Information). Collectively, these data indicate the existence of a single chemical environment around the Ln^{3+} ion in each case. The pertinent values are summarized in Table 2.

On the basis of the room-temperature emission spectra and on the lifetime measurements, we can estimate the intrinsic quantum yield (η) of the $^5\text{D}_0 \rightarrow ^7\text{F}_1$ ion excited state.²² The luminescence decay lifetime (τ) is directly related to the radiative and nonradiative decay rates of the lanthanide ion. The radiative lifetime (τ_{rad}) can be calculated using eq 1, assuming that the energy of the $^5\text{D}_0 \rightarrow ^7\text{F}_1$ transition (MD) and its oscillator strength are constant²³

$$A_{\text{RAD}} = 1/\tau_{\text{rad}} = A_{\text{MD},0} n^3 (I_{\text{tot}}/I_{\text{MD}}) \quad (1)$$

where, $A_{\text{MD},0}$ (14.65 s^{-1}) is the spontaneous emission probability of the $^5\text{D}_0 \rightarrow ^7\text{F}_1$ transition in vacuo, $I_{\text{tot}}/I_{\text{MD}}$ is the ratio of the total area of the corrected Eu^{3+} emission spectrum to the area of the $^5\text{D}_0 \rightarrow ^7\text{F}_1$ band, and n is the refractive index of the medium. An average index of refraction equal to 1.5 was considered.²⁰ Lifetime (τ), radiative (A_{RAD}) and nonradiative (A_{NR}) transition rates are related to through the following eq 2 where A_{RAD} can be obtained by summing over the radiative rates

$$1/\tau_{\text{obs}} = A_T = A_{\text{RAD}} + A_{\text{NR}} \quad (2)$$

A_{NR} for each $^5\text{D}_0 \rightarrow ^7\text{F}_j$ transition. Assuming that nonradiative and radiative processes are essentially involved in the depopulation of $^5\text{D}_0$ state, the intrinsic quantum yield η can be expressed as

$$\eta = (A_{\text{RAD}}/A_{\text{RAD}} + A_{\text{NR}}) \quad (3)$$

The parameters A_{RAD} , A_{NR} , and the intrinsic quantum yield values (η) for the Eu^{3+} complexes are shown in the Table 2. It is evident from these values that $\text{Eu}(\text{acac})_3(\text{m-PPV})$ exhibits higher $^5\text{D}_0$ lifetime and intrinsic quantum yield as compared to $\text{Eu}(\text{acac})_3(\text{OPV})$.

Effect of Copolymer and Spacer Effect on the Photosensitization of Ln^{3+} Ions. The effect of polymer structure on the photosensitizing of Tb^{3+} and Eu^{3+} ions was also investigated and the results are depicted in Figure S28a, S28b and Table S2 in Supporting Information. The results clearly highlights that the sensitization efficiency of Ln^{3+} ion with various polymeric materials increases in the order p-PPV < co-PPV < m-PPV (see Figure S28 in Supporting Information). Thus it can be concluded that m-PPV is a better sensitizer for Eu^{3+} or Tb^{3+} due to the superior match of the triplet energy level with that of emitting levels of the Ln^{3+} ions. On the other hand, p-PPV shows poor sensitization for Ln^{3+} ions due to its extended conjugation, which in turn decreases the triplet energy level ($19\ 000 \text{ cm}^{-1}$) (see Figure S29 in Supporting Information). Thus the triplet energy level lies less than the emitting level of $^5\text{D}_4$ of Tb^{3+} and hence it cannot sensitize Tb^{3+} ion. In the case of Eu^{3+} , poor sensitization has been noticed with p-PPV in view of the lower energy gap ($\Delta E = ^3\pi\pi^* - ^5\text{D}_1 = 1500 \text{ cm}^{-1}$), which can facilitate back energy transfer process. Because of decrease in conjugation, co-PPV sensitizes Eu^{3+} better than p-PPV. The triplet energy level of co-PPV $19\ 600 \text{ cm}^{-1}$ (see Figure S29 in Supporting Information) lies well above the emitting level of $^5\text{D}_0$ of Eu^{3+} . On the other hand, co-PPV triplet energy level lies below $^5\text{D}_4$ level of Tb^{3+} and hence it cannot sensitize Tb^{3+} ion. To study the effect of spacer length between the polymer backbone to the Ln^{3+} metal ion center, a new carboxylic acid functionalized poly(*m*-phenylenevinylene) bearing shorter spacer (one carbon atom less) was synthesized starting from 3-(4-hydroxyphenyl)acetic acid (see Supporting Information for detail synthesis). This new polymer m-PPV-A (A refers to acetic acid) was also complexed with Tb^{3+} and Eu^{3+} under the identical conditions. The PL-spectra of the Tb^{3+} and Eu^{3+} complexes of m-PPV-A were recorded by exciting at 310 nm and are shown in Figures S28c and S28d in Supporting Information. The photosensitization efficiency of Ln^{3+} ion with m-PPV-A is found to be same as that of m-PPV (see Table S3 and Figure S28 in Supporting Information). This suggests that the reducing the length of the spacer did not showed any appreciable changes in the emission properties of these Ln^{3+} complexes.

Conclusion

In conclusion, new classes of carboxylic-functionalized poly(*m*-phenylenevinylene)s were synthesized and utilized as photosensitizers for tuning the color of lanthanide complexes. The present investigation has the following important outcomes: (i) novel blue light emitting oligo and poly(*m*-phenylenevinylene)s were developed starting from phenyl propanoic and phenyl acetic acids via witting polycondensation reactions, (ii) Eu^{3+} and Tb^{3+} lanthanide complexes were successfully prepared for these conjugated materials and characterized by NMR, FT-IR and MALDI-TOF, (iii) m-PPV polymer was found efficient

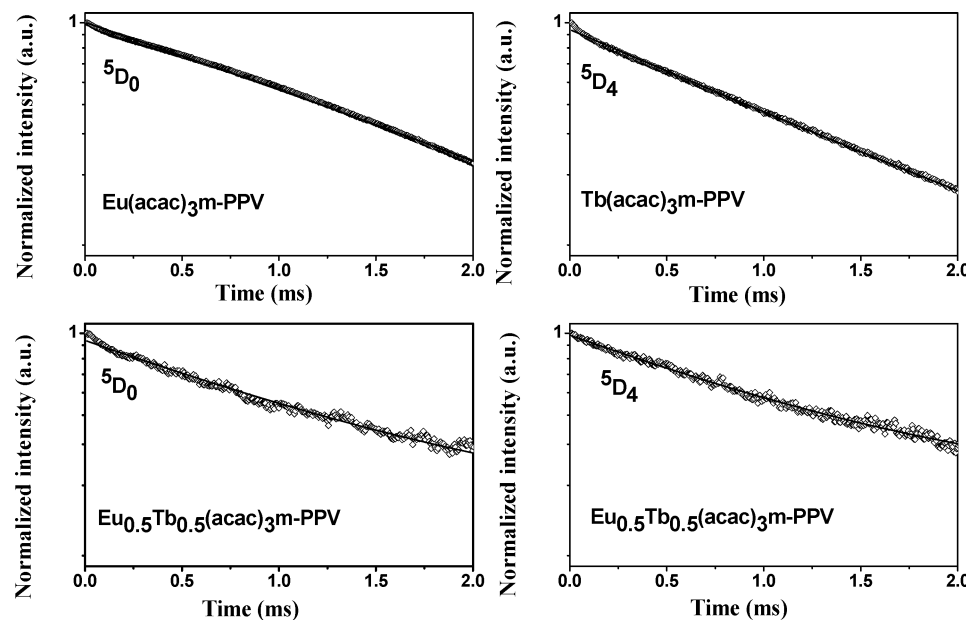


Figure 9. Decay profiles of the Ln^{3+} complexes with m-PPV.

TABLE 2: Photophysical Parameters of the Complexes

| complexes | τ (ms) | | $I_{0,1}/I_{0,2}$ | A_{RAD} (s^{-1}) | A_{NR} (s^{-1}) | η (%) |
|-------------------------------------|-----------------|-----------------|-------------------|------------------------|-----------------------|------------|
| | 5D_0 | 5D_4 | | | | |
| $Eu(acac)_3(H_2O)$ (OPV) | 0.82 ± 0.07 | | 11.00 | 298 | 914 | 24 |
| $Eu(acac)_3$ (m-PPV) | 1.53 ± 0.04 | | 5.34 | 415 | 240 | 63 |
| $Tb(acac)_3(H_2O)$ (OPV) | | 1.32 ± 0.06 | | | | |
| $Tb(acac)_3$ (m-PPV) | | 1.19 ± 0.04 | | | | |
| $Eu_{0.5}Tb_{0.5}(acac)_3(m-PPV)$ | 1.33 ± 0.05 | 1.17 ± 0.05 | | | | |
| $Eu_{0.5}Tb_{0.5}(acac)_3(m-PPV-A)$ | 1.12 ± 0.05 | 1.20 ± 0.04 | | | | |

photosensitizer for both Eu^{3+} and Tb^{3+} ions and produced sharp magenta and sky blue colors, respectively, whereas its small oligomer counterpart (m-OPV) failed as sensitizer, (iv) the partial blue emission of the m-PPV in combination with Tb^{3+} and Eu^{3+} ions in a single system produce white emission exhibited a novel white emission color with CIE 1976 color coordinates $x = 0.28$, $y = 0.34$, and (v) the effect of spacer length between the metal center to conjugated backbone as well as copolymer constituents were also investigated. The m-PPV conjugated polymer design provides a new opportunity for tuning the color of the lanthanide complexes that may find potential applications in optoelectronics. Currently, the research work in progress to tune the polymer structures for producing high molecular weight polymers as well as bright emission colors. These materials will be tested in collaboration with device fabrication groups. To summarize, in the present investigation for the first time a new carboxylic acid functionalized poly(*m*-phenylenevinylene)s were synthesized to tune the red, green, and white colors of the lanthanide complexes in a single polymeric system and the mechanistic aspects of the energy transfer process were investigated in detail using photophysical techniques.

Acknowledgment. We thank Department of Science of Technology, New Delhi, India under Scheme NSTI Programme-SR/S5/NM-06/2007 for financial support. M.L.P.R. thanks CSIR, New Delhi, Indian (CSIR-NWP-010) for the financial support. A.B. thanks CSIR-New Delhi, India for Junior Research Fellowship.

Supporting Information Available: The structural characterization data of monomers by 1H -NMRs, IR, and HR-MS

spectra, emission spectrum of $Eu(acac)_3(m-PPV-A)$ at multiple excitation wavelength, and CIE coordinate diagram of m-PPV-A complexes. This material is available free of charge via the Internet at <http://pubs.acs.org>.

References and Notes

- (1) Burroughes, J. H.; Bradley, D. D. C.; Brown, A. R.; Marks, R. N.; MacKay, K.; Friend, R. H.; Burn, P. L.; Holmes, A. B. *Nature* **1990**, *347*, 539.
- (2) (a) Forrest, S. R. *Nature* **2004**, *428*, 911. (b) Gustafsson, G.; Cao, Y.; Treasy, G. M.; Klavetter, F.; Colaneri, N.; Heeger, A. J. *Nature* **1992**, *357*, 477.
- (3) (a) Segal, M.; Baldo, M. A.; Holmes, R. J.; Forrest, S. R.; Soos, Z. G. *Phys. Rev. B* **2003**, *68*, 075211/1. (b) Kido, J.; Okamoto, Y. *Chem. Rev.* **2002**, *102*, 2357. (c) Amrutha, S. R.; Jayakannan, M. *J. Phys. Chem. B* **2006**, *110*, 4083. (d) Amrutha, S. R.; Jayakannan, M. *J. Phys. Chem. B* **2008**, *112*, 1119. (e) Amrutha, S. R.; Jayakannan, M. *Macromolecules* **2007**, *40*, 2380. (f) Liao, L.; Pang, Y.; Ding, L.; Karasz, F. E. *Macromolecules* **2002**, *35*, 3819. (g) Pang, Y.; Li, J.; Hu, B.; Karasz, F. E. *Macromolecules* **1999**, *32*, 3946. (h) Liao, L.; Pang, Y.; Ding, L.; Karasz, F. E. *Macromolecules* **2001**, *34*, 6756. (i) Zheng, M.; Sarker, A. M.; Gurel, E. E.; Lahti, P. M.; Karasz, F. E. *Macromolecules* **2000**, *33*, 7426. (j) Anish, C.; Amrutha, S.; Jayakannan, M. *J. Polym. Sci., Part A: Polym. Chem.* **2008**, *46*, 3241–3256. (k) Resmi, R.; Amrutha, S. R.; Jayakannan, M. *J. Polym. Sci., Part A: Polym. Chem.* **2009**, *47*, 2631–2341. (l) Balamurugan, A.; Reddy, M. L. P.; Jayakannan, M. *J. Polym. Sci., Part A: Polym. Chem.* **2009**, *47*, 5144–5157.
- (4) (a) Chen, X. Y.; Yang, X.; Holliday, B. J. *J. Am. Chem. Soc.* **2008**, *130*, 1546. (b) Ling, Q. D.; Kang, E. T.; Neoh, K. G. *Macromolecules* **2003**, *36*, 6995. (c) Pei, J.; Liu, X. L.; Yu, W. L.; Lai, Y. H.; Niu, Y. H.; Cao, Y. *Macromolecules* **2002**, *35*, 7274.
- (5) (a) de Bettencourt-Dias, A. *Dalton Trans.* **2007**, 2229. (b) Piguet, C.; Bunzli, J. C. G. *Chem. Soc. Rev.* **2005**, *34*, 1048. (d) Parker, D.; Williams, J. A. G. *The Lanthanides and Their Interrelation with Biosystems*; M. Dekker, Inc.: New York, 2003; Vol. 40, p 233. (e) Kuriki, K.; Koike, Y.; Okamoto, Y. *Chem. Rev.* **2002**, *102*, 2347. (f) Brunet, E.; Juanes, O.; Rodriguez-Ubis, J. C. *Curr. Chem. Biol.* **2007**, *1*, 11. (g) Evans, R. C.; Douglas, P.; Winscom, C. J. *Coord. Chem. Rev.* **2006**, *250*, 2093.

- (6) (a) Evans, R. C.; Douglas, P.; Winscom, C. J. *Coord. Chem. Rev.* **2006**, *250*, 2093. (b) Bünzli, J.-C. G.; Piguet, C. *Chem. Rev.* **2002**, *102*, 1897. (c) de Sa, G. F.; Malta, O. L.; de Mello Donega, C.; Simas, A. M.; Longo, R. L.; Santa-Cruz, P. A.; da Silva, E. F., Jr. *Coord. Chem. Rev.* **2000**, *196*, 165.
- (7) Sabbatini, N.; Guardigli, M.; Lehn, J. M. *Coord. Chem. Rev.* **1993**, *123*, 201.
- (8) (a) Pavithran, R.; Saleesh Kumar, N. S.; Biju, S.; Reddy, M. L. P.; Junior, S. A.; Freire, R. O. *Inorg. Chem.* **2006**, *45*, 2184. (b) Remya, P. N.; Biju, S.; Reddy, M. L. P.; Cowley, A. H.; Findlater, M. *Inorg. Chem.* **2008**, *47*, 7396. (c) Ambili Raj, D. B.; Biju, S.; Reddy, M. L. P. *Inorg. Chem.* **2008**, *47*, 8091. (d) Biju, S.; Reddy, M. L. P.; Cowley, A. H.; Vasudevan, K. V. *J. Mater. Chem.* **2009**, *19*, 5179. (e) Binnemanns, K. *Handbook on the Physics and Chemistry of Rare Earths*; Elsevier: Amsterdam, 2005; Chapter 225, vol. 35, pp 107–272. (f) Binnemanns, K.; Lenaerts, P.; Driesen, K.; Walrand, G. C. *J. Mater. Chem.* **2004**, *14*, 191. (g) Biju, S.; Ambili Raj, D. B.; Reddy, M. L. P.; Kariuki, B. M. *Inorg. Chem.* **2006**, *45*, 10651.
- (9) (a) Shyni, R.; Biju, S.; Reddy, M. L. P.; Cowley, A. H.; Findlater, M. *Inorg. Chem.* **2007**, *46*, 11025. (b) Shyni, R.; Reddy, M. L. P.; Cowley, A. H.; Findlater, M. *Eur. J. Inorg. Chem.* **2008**, *4387*.
- (10) (a) Biju, S.; Ambili Raj, D. B.; Reddy, M. L. P.; Jayasankar, C. K.; Cowley, A. H.; Findlater, M. *J. Mater. Chem.* **2009**, *19*, 1425. (b) Lidia Armelao, L.; Bottaro, G.; Quici, S.; Cavazzini, M.; Concetta Raffo, M.; Barigelli, F.; Accorsi, G. *Chem. Commun.* **2007**, 2911.
- (11) (a) Virgili, T.; Lidzey, D. G.; Bradley, D. D. C. *Adv. Mater.* **2000**, *12*, 58. (b) Nigel, A. H. M.; Salata, O. V.; Christou, V. *Synth. Met.* **2002**, *126*, 7. (c) Peng, J. B.; Takada, N.; Minami, N. *Thin Solid Films* **2002**, *405*, 224. (d) Liang, C. J.; Li, W. L.; Yu, J. Q.; Liu, X. Y.; Li, D.; Zhao, Y.; Peng, J. B. *Chin. J. Lumin.* **1996**, *17*, 382. (e) Uekawa, M.; Miyamoto, Y.; Ikeda, H.; Kaifu, K.; Nakaya, T. *Bull. Chem. Soc. Jpn.* **1998**, *71*, 2253. (12) Segura, J. L. *Acta Polym.* **1998**, *49*, 319.
- (13) McGehee, M. D.; Bergstedt, T.; Zhang, C.; Saab, A. P.; O'Regan, M. B.; Bazan, G. C.; Srdanov, V. I.; Heeger, A. J. *Adv. Mater.* **1999**, *11*, 1349.
- (14) (a) Li, Q.; Li, T.; Wu, J. *J. Phys. Chem. B* **2001**, *105*, 12293. (b) Cheng, Y.; Zou, X.; Zhu, D.; Zhu, T.; Liu, Y.; Zhang, S.; Huang, H. *J. Polym. Sci., Part A: Polym. Chem.* **2007**, *45*, 650. (c) Zhang, Z. H.; Yuan, J. B.; Tang, H. J.; Tang, H.; Wang, L. N.; Zhang, K. L. *J. Polym. Sci., Part A: Polym. Chem.* **2009**, *47*, 210. (d) Yang, M.; Ling, Q.; Hiller, M.; Fun, X.; Liu, X.; Wang, L.; Zhang, W. *J. Polym. Sci., Part A: Polym. Chem.* **2000**, *38*, 3405. (e) Shunmugam, R.; Tew, G. N. *Polym. Adv. Technol.* **2007**, *18*, 940.
- (15) Shunmugam, R.; Tew, G. N. *Polym. Adv. Technol.* **2008**, *19*, 596.
- (16) (a) Carnall, W. T. *In Handbook on the Physics and Chemistry of Rare Earths*; Gschneidner, K. A., Eyring, L., Eds.; Elsevier: Amsterdam, The Netherlands, 1987; Vol. 3, Chapter 24, p 171. (b) Dieke, G. H. *Spectra and Energy Levels of Rare Earth Ions in Crystals*; Interscience: New York, 1968. (c) Biju, S.; Ambili Raj, D. B.; Reddy, M. L. P.; Kariuki, B. M. *Inorg. Chem.* **2006**, *45*, 10651. (d) Klink, S. I.; Grave, L.; Reinhoudt, D. N.; vanVegel, F. C. J. M.; Werts, M. H. V.; Geurts, F. A. J.; Hofstraat, J. W. *J. Phys. Chem. A* **2000**, *104*, 5457.
- (17) (a) Carlos, L. D.; Messaddeq, Y.; Brito, H. F.; Sa Ferreria, R. A.; de Zea Bermudez, V.; Ribeiro, S. J. L. *Adv. Mater.* **2000**, *12*, 594. (b) Fernandes, J. A.; Ferreira, R. A. S.; Pillinger, M.; Carlos, L. D.; Goncalves, I. S.; Ribeiro-Claro, P. J. A. *Eur. J. Inorg. Chem.* **2004**, 3913. (c) Peng, C.; Zhang, H.; Yu, J.; Meng, Q.; Fu, L.; Li, H.; Sun, L.; Guo, X. *J. Phys. Chem. B* **2005**, *109*, 15278.
- (18) (a) Shi, M.; Li, F.; Yi, T.; Zhang, D.; Hu, H.; Huang, C. *Inorg. Chem.* **2005**, *44*, 8929. (b) Xin, H.; Shi, M.; Gao, X. C.; Huang, Y. Y.; Gong, Z. L.; Nie, D. B.; Cao, H.; Bian, Z. Q.; Li, F. Y.; Huang, C. H. *J. Phys. Chem. B* **2004**, *108*, 10796. (c) Oxley, D. S.; Walters, R. W.; Copenhagen, J. E.; Meyer, T. Y.; Petoud, S.; Edenborn, H. M. *Inorg. Chem.* **2009**, *48*, 6332.
- (19) Latva, M.; Takalo, H.; Mukkala, V. M.; Matachescu, C.; Rodriguez-Ubis, J. C.; Kanakare, J. *J. Lumin.* **1997**, *75*, 149.
- (20) Steemers, F. J.; Verboom, W.; Reinhoudt, D. N.; Vander Tol, E. B.; Verhoeven, J. W. *J. Am. Chem. Soc.* **1995**, *117*, 9408.
- (21) You, B.; Kim, H. J.; Park, N. G.; Kim, Y. S. *Bull. Korean Chem. Soc.* **2007**, *22*, 1005.
- (22) Molina, C.; Moreira, P. J.; Gonçalves, R. R.; Sa' Ferreira, R. A.; Messaddeq, Y.; Ribeiro, S. J. L.; Soppera, O.; Leite, A. P.; Marques, P. V. S.; de Zea Bermudez, V.; Carlos, L. D. *J. Mater. Chem.* **2005**, *15*, 3937.
- (23) Roesky, H. W.; Andruh, M. *Coord. Chem. Rev.* **2003**, *236*, 91.

JP9067312